ELSEVIER

Journal of Photochemistry and Photobiology A: Chemistry 155 (2003) 79–91

Journal of Photochemistry and Photobiology A:Chemistry

www.elsevier.com/locate/jphotochem

A study of the strongly fluorescent species formed by the interaction of the dye 1,4-dihydroxyanthraquinone (quinizarin) with Al(III)

Luisa Quinti [a], Norman S. Allen [a,*], Michele Edge [a], Brian P. Murphy [a], Angelo Perotti [b]

[a] *Department of Chemistry and Materials, Manchester Metropolitan University, Chester Street, Manchester, M1 5GD, UK*
[b] *Dipartimento di Chimica Generale, Università di Pavia, Via Taramelli 12, 27100 Pavia, Italy*

Received 16 July 2002; received in revised form 17 September 2002; accepted 19 September 2002

Abstract

Strongly fluorescent species form when Al(III) ions interact with 1,4-dihydroxyanthraquinone (quinizarin, QNZ), in aqueous and non-aqueous media. Speciation studies suggest the supramolecular and/or polymeric nature of these complexes as both their absorbance and fluorescence intensity increase proportionally to the Al(III) equivalents up to 60/1 Al(III)/QNZ and in certain cases even further.

iso-Propanol is the solvent that yields the highest quantum yield of fluorescence ($\Phi = 0.51$ for QNZ/Al(III) 1/75). Counterion effects were also studied and $Al(acac)_3$ was found to be the compound with which the highest quantum yield values were obtained, suggesting an active role for $acac^-$ in the stabilisation of the QNZ/Al(III) fluorescent species.

Potentiometric studies, performed between pH 3 and 6 in dioxane/water 80/20, suggest the formation of 2/1 QNZ/Al(III) species, having global stability constant of 10^{40}. Studies at higher ratios of Al(III) were precluded by precipitations.

Keywords: Quinizarin; Hydroxyanthraquinones; Aluminium; Fluorescence; Supramolecular complexes

1. Introduction

1,4-Dihydroxyanthraquinone (quinizarin, QNZ) is accredited with properties that span from being used as a fungicide and pesticide, to being employed as a dye, a photoinitiator and an additive in lubricants [1]. It also serves as a model for anthracycline antitumour antibiotics [2]. Significantly, the fluorescent complexes of quinizarin with lithium and boron ions are used as spectrophotometric analytical reagents for these metals [3,4].

The literature on the speciation of quinizarin complexes is not mature [5,6]. Early reports suggest the formation of non-polymeric species, having 1/1, 1/2 or 1/3 metal/QNZ stoichiometry [6–8]. In contrast, recent reports cite the formation of polymeric complexes with 1/1 or 2/3 metal/QNZ ratio [1,5,9,10]. The most commonly proposed structures for quinizarin complexes are shown in Fig. 1.

The only X-ray crystal structure is that of the tertiary complex $[Fe_2(QNZ^{-2H})(salen)_2]$ where quinizarin is bridging between two Fe(III) ions, confirming its binucleating coordination ability [11]. The two hydroxyquinone groups of quinizarin coordinate to two different Fe(III) ions and the remaining coordination sites on each metal are occupied by the salen donors (salen = bis(salicylidene)ethylene diamine).

Strongly fluorescent species form when Al(III) and quinizarin are present in aqueous and non-aqueous media. Work reported by this group more than 10 years ago revealed that the fluorescence of the Al(III) complexes increased proportionally with the ratio of Al(III)/QNZ up to 10/1. Furthermore, these complexes demonstrated photoconductive properties [12,13]. Such complexes offer potential as fluorescent sensors and in LED devices; similar complexes are known to be of great potential in these areas [3].

This research aims to give further insight into the nature of these species, thought to be complexes of Al(III) and quinizarin. This work will also report kinetic and thermodynamic studies of the photoactive species and the current progresses into the isolation of the photoactive complexes.

2. Results and discussion

2.1. Preliminary solution studies

The effect of Al(III) ions, and any influence of counterion in determining speciation and fluorescence, was determined through the use of the following/ $Al(acac)_3$;

* Corresponding author.
E-mail address: n.allen@mmu.ac.uk (N.S. Allen).

1010-6030/02/$ – see front matter © 2002 Elsevier Science B.V. All rights reserved.
PII: S1010-6030(02)00360-X

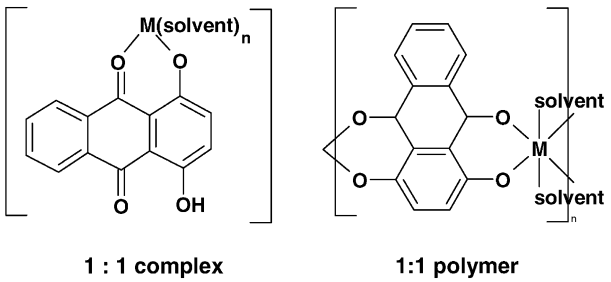

Fig. 1. Schematic representation of the structure of the QNZ complexes reported in the literature.

$Al(NO_3)_3{\cdot}9H_2O$; $AlCl_3$; $Al(ClO_4)_3{\cdot}9H_2O$. The choice of the Al(III) precursors necessarily limited the range of solvents that could be used due to solubility problems. In this respect $Al(acac)_3$ was found to be the best compound for solution studies because it dissolves in a range of alcohols: methanol; ethanol; propanol; *iso*-propanol; butanol; *tert*-butanol.

Fig. 2 shows UV-Vis spectra for QNZ and for QNZ/Al(III) at different molar ratios. The QNZ solutions have a yellow-orange colour that depends on the solvent, and their UV-Vis spectra are characterised by a broad band centred at ca. 480 nm. Upon progressive addition of Al(III), the development of a strongly fluorescent pink colouration occurred. This corresponded, in UV-Vis spectroscopy, with the disappearance of the broad band at 480 nm, that became a shoulder centred at ca. 500 nm, and with the appearance of two bands having maxima at, respectively, ca. 530 and 560 nm. When QNZ/Al(III) molar ratios were lower than 1/5, the band at 530 nm had higher absorbance than that at 560 nm; at with higher equivalents of Al(III), the band at 560 nm had a higher absorbance.

Typical fluorescence spectra of the QNZ/Al(III) species that formed in solution while increasing the metal molar ratio, are reported in Fig. 3. The formation of the pink colour resulted in the formation of two bands and a shoulder centred, respectively, at ca. 570, 610 and 650 nm. When QNZ/Al(III) molar ratios were lower than 1/5, the two bands at 570 and 610 nm had the same intensity while with higher ratios of Al(III), the band at 570 nm exhibited a higher intensity.

2.2. Time measurements

With all the solvents the formation of the pink colour upon addition of Al(III) to quinizarin occurred after some time. The spectra evolved from an initial spectrum analogous to that of pure QNZ, to a final spectrum whose character depended on the QNZ/Al(III) molar ratio, in analogy to those in Fig. 2.

From qualitative kinetic studies, performed using both UV-Vis and fluorescence spectroscopy, it was concluded that the pink colour developed in the first 20–30 min after the mixing of metal and ligand. After this interval of time, both absorbance and fluorescence intensity slowly approached an equilibrium value (as shown in Fig. 4). Therefore, 90 min from the mixing of the reagents was estimated as a reasonable interval of time after which the recording of the spectra was not unduly affected by equilibration.

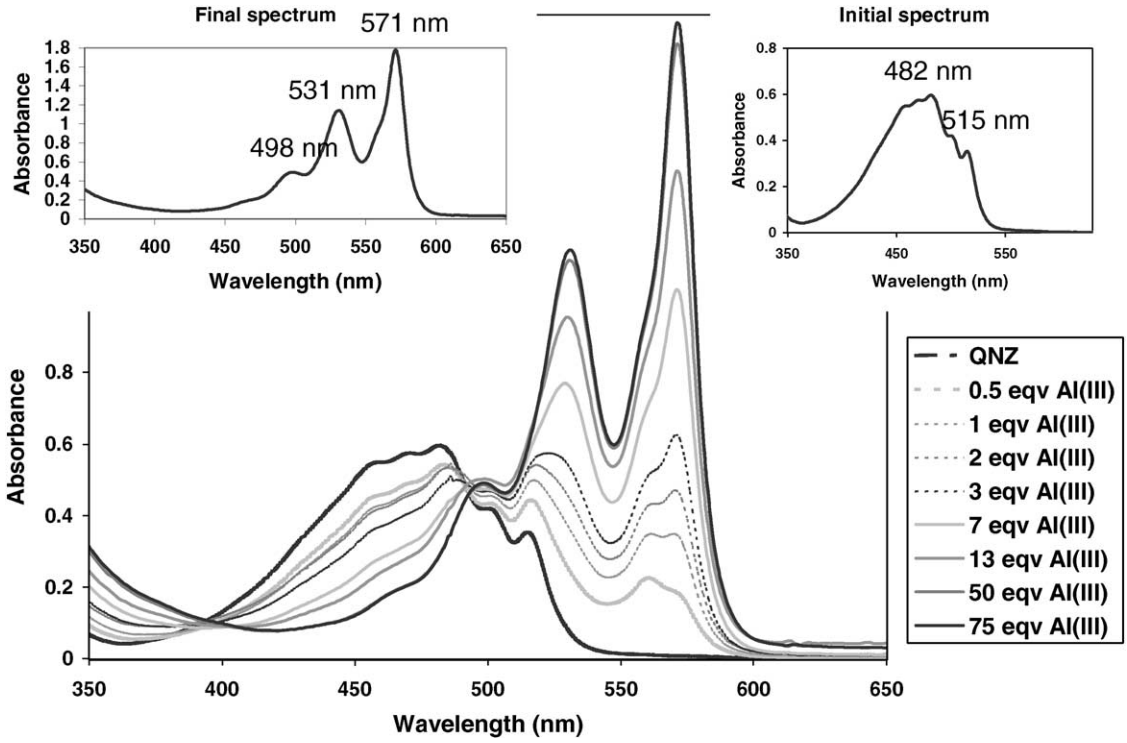

Fig. 2. UV-Vis spectra for quinizarin and QNZ/$Al(acac)_3$ at different molar ratios in *i*-PrOH.

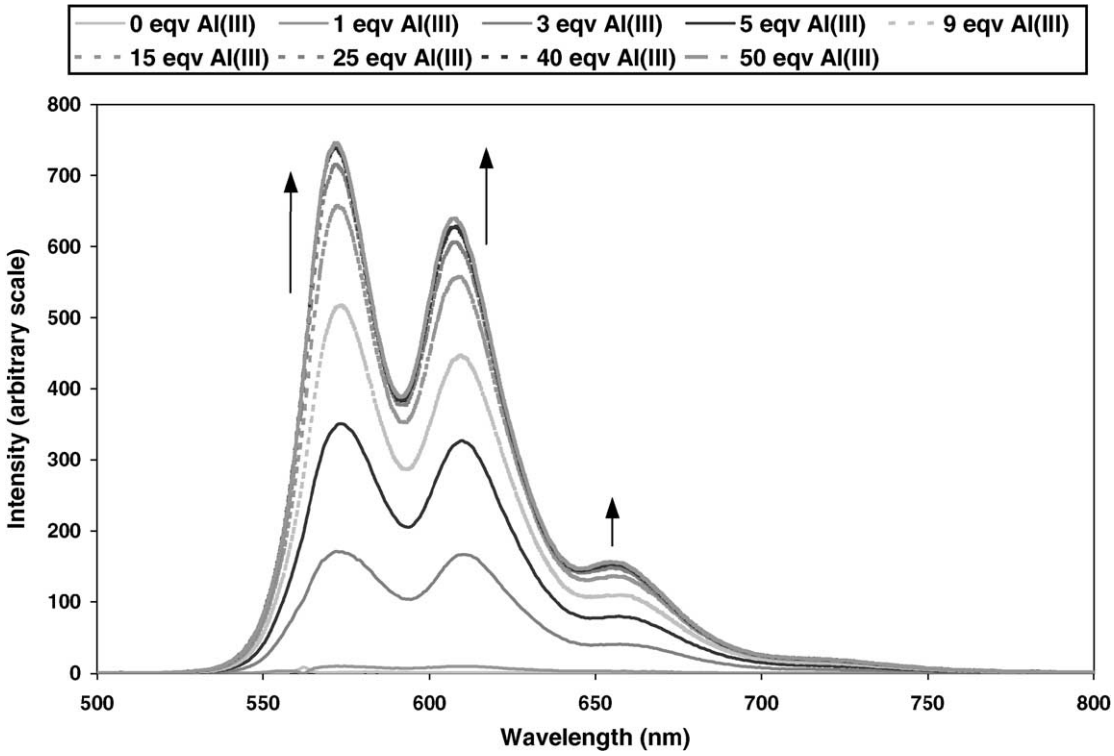

Fig. 3. Fluorescence spectra from the titration of QNZ with $Al(ClO_4)_3$ in MeOH up to 50 equiv. Al(III) ($\lambda_{exc} = 530$ nm).

All the spectra reported in this work were recorded after equilibration of the solutions had occurred.

2.3. Speciation studies

The speciation of the fluorescent species that formed in solution was investigated using optical methods such as the continuous variation (or Job's method) and the mole ratio. Examples of these experiments are shown in Figs. 2 and 3. In titrations, Al(III) was added to QNZ up to of 75/1 metal/ligand ratio. These solution studies suggested that the species forming in solution were supramolecular assemblies. In fact, both absorbance and fluorescence intensity were found to increase proportionally with the ratio of

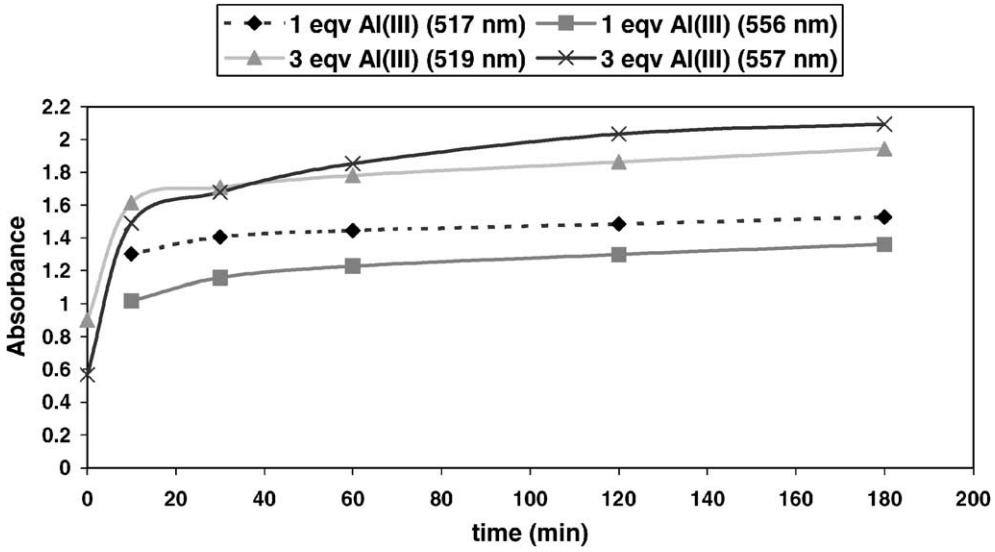

Fig. 4. Studies of the absorbance of QNZ/$Al(ClO_4)_3 \cdot 9H_2O$ in MeOH vs. time.

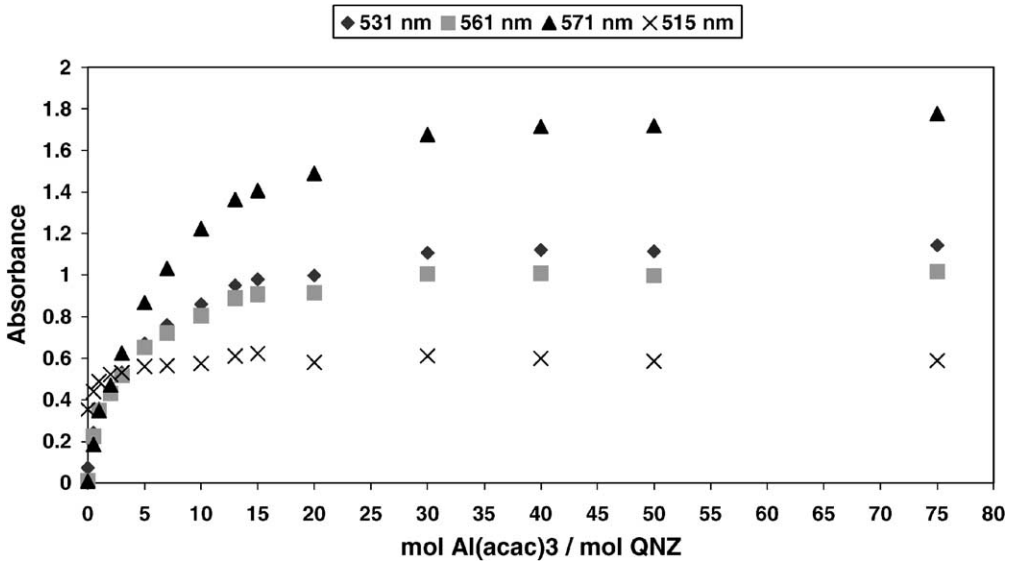

Fig. 5. Titration of quinizarin with $Al(acac)_3$ in *i*-PrOH followed by UV-Vis spectroscopy.

aluminium-to-quinizarin up to ratios of 60/1, as shown in Figs. 5 and 6. In some instances enhanced fluorescence was found even at higher ratios.

The difficulty in recovering quinizarin complexes, described in more detail later, and the poor quality of the characterisation data available from the literature make reasonable the hypothesis of supramolecular complexes forming.

2.4. Temperature effect

UV-Vis studies of 1/1, 3/1 and 5/1 Al(III)/QNZ solutions at 298 and 323 K, revealed that temperature does not influence the formation of the fluorescent species.

2.5. Solvent effect

In evaluating any solvent effect on fluorescence quantum yields, $Al(acac)_3$ was the favoured source of Al(III) because of solubility requirements. The solvents investigated were methanol, ethanol, propanol, *iso*-propanol, butanol and *tert*-butanol. Previous work from this group had shown an increase in luminescence in proportion to the Al(III)/QNZ ratio [13]. Therefore, attention was mainly focussed on the following three Al(III)/QNZ ratios/ 20/1, 40/1 and 75/1. The trends for PrOH, *i*-PrOH and BuOH are reported in Fig. 7. Even at these high metal/QNZ ratios, quantum yields were found to increase proportionally with the Al(III) ratio.

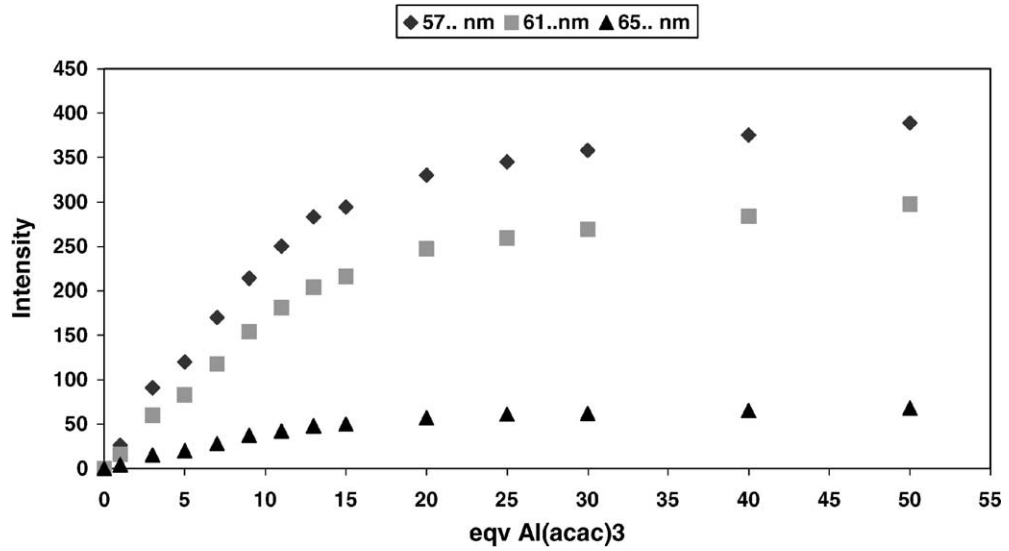

Fig. 6. Titration of quinizarin with $Al(acac)_3$ in MeOH followed by fluorescence.

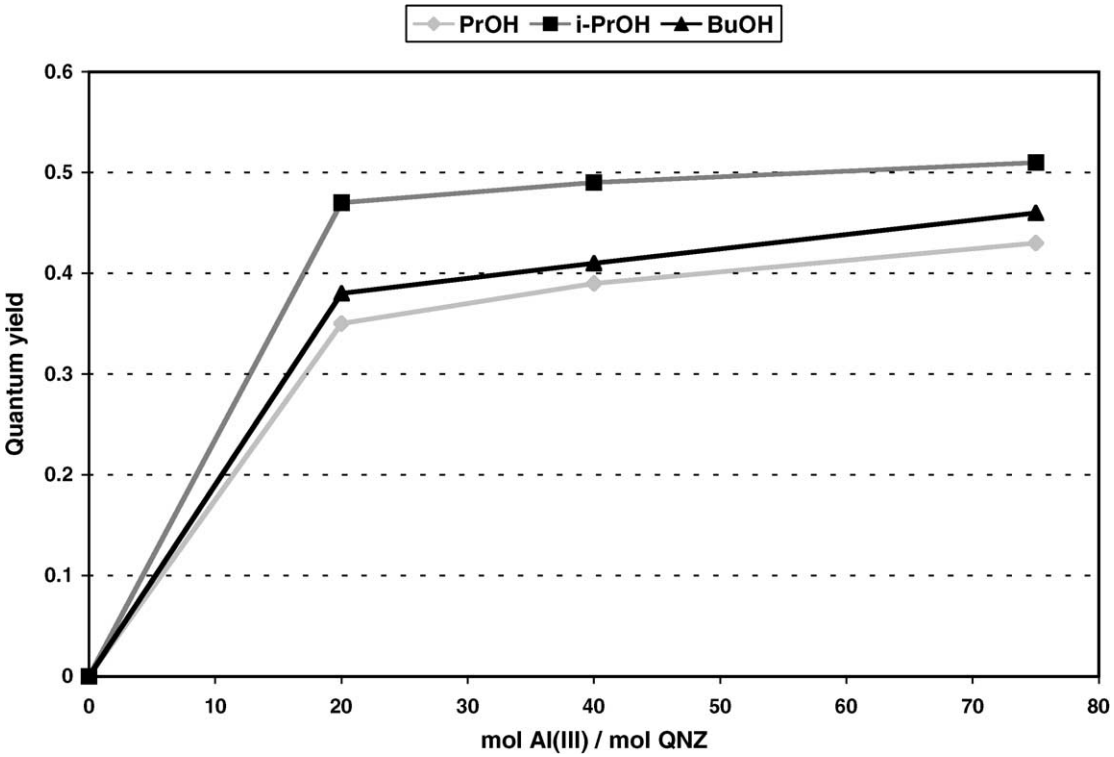

Fig. 7. Quantum yield values for different QNZ/Al(acac)$_3$ ratios.

Considering the solvent effect, the following trend for the quantum yield values was found with all three Al(III)/QNZ ratios/ *i*-PrOH > BuOH ≥ PrOH > EtOH > *t*-BuOH > MeOH, while the values spanned from 0.17 with MeOH to 0.51 with *i*-PrOH. Fig. 8 shows the quantum yield values of the 75/1 Al(acac)$_3$/QNZ ratio for all the alcohols.

As aforementioned, upon addition of the colourless Al(III) solutions to the yellow-orange quinizarin solutions in the solvent of choice, an orange/pink fluorescent colour developed. The intensity and hue of the pink colour depended on the solvent. A correlation of the quantum yield values versus a function of the solvent dielectric constant, *D*, is shown in Fig. 9. With solvents more polar than *i*-PrOH, a decrease in the quantum yield values was found. This suggested that a certain degree of polarisation of the first excited singlet state took place in solution with polar alcohols. Nevertheless, the plot of λ_{max} of absorbance and fluorescence emission versus *f*(*D*) (not reported) showed the expected linear trend [14]. The maximum wavelengths of absorption and emission for

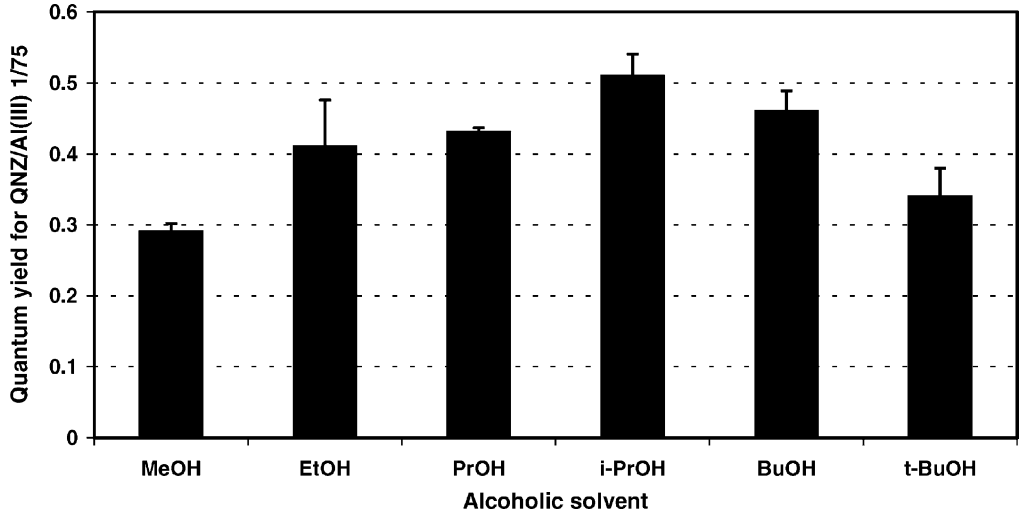

Fig. 8. Quantum yield values for QNZ/Al(acac)$_3$ 1/75 in different alcoholic solvents. Rhodamine B in EtOH has been used as reference ($\Phi = 0.70$).

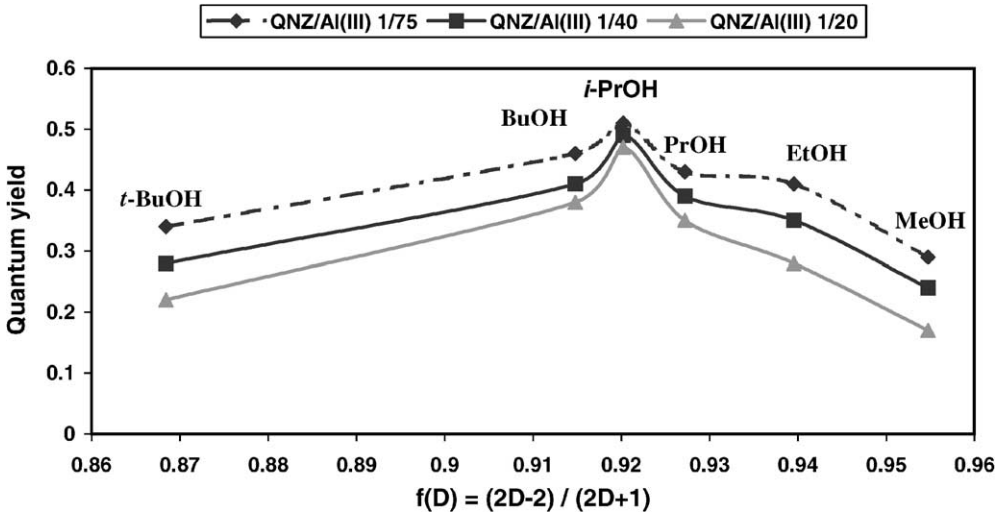

Fig. 9. Plot of quantum yields for QNZ/Al(acac)$_3$ vs. $2D-2/2D+1$, where D is the solvent dielectric constant. Note: the tabulated value for D of *tert*-butanol used in the calculations was given at 30 °C while for all the other solvents the values used were given at 25 °C.

QNZ/Al(acac)$_3$ 1/40 in the different alcohols are reported in Table 1.

2.6. Counterion effect

Evidence for any counterion effect was investigated in EtOH comparing the quantum yield values obtained with Al(acac)$_3$, Al(NO$_3$)$_3$·9H$_2$O, AlCl$_3$ and Al(ClO$_4$)$_3$·9H$_2$O. 1/20, 1/40 and 1/75 QNZ/Al(III) molar ratios were investigated. As Fig. 10 shows, the quantum yield values for the first two ratios reflect the different acidity of the Al(III) materials and their degree of dissociation in solution. The highest quantum yield values with the first two ratios were given by Al(acac)$_3$. When the QNZ/Al(III) stoichiometry was 1/75, instead, the quantum yield values were found to be similar with all the four Al(III) compounds. Table 2 reports the maximum wavelengths of absorption and emission for QNZ/Al(III) 1/40 in EtOH.

2.7. pH effect

When NaOH was added to solutions of QNZ, in QNZ/OH$^-$ =1/7 ratio, the QNZ solutions became immediately violet, due to the formation of phenolate ions.

Table 1
Comparison of the maximum wavelengths of absorbance and emission for QNZ/Al(acac)$_3$ 1/40 in different alcohols

Solvent	Maximum absorbance (nm)	Maximum emission (nm)
MeOH	570	575
EtOH	569	576
PrOH	571	577
i-PrOH	571	577
BuOH	572	578
t-BuOH	571	576

Table 2
Comparison of the maximum wavelengths of absorbance and emission for QNZ/Al(III) 1/40 in EtOH

Al(III) compound	Maximum absorbance (nm)	Maximum emission (nm)
Al(acac)$_3$	571	577
Al(NO$_3$)$_3$	561	575
AlCl$_3$	561	573
Al(ClO$_4$)$_3$	560	573

Nevertheless, with time their colour became pink (but not fluorescent) and then yellow. Qualitative UV-Vis kinetic studies show the gradual conversion of the spectra back to that of neutral QNZ while the UV-Vis spectrum of the violet solution has its maximum of absorbance at 559 nm, with a shoulder at 580 nm. Therefore, strong bases are able to rapidly deprotonate QNZ but the deprotonated species are unstable in solution and they convert back to the protonated form by extracting the necessary protons from protic solvent molecules. Weaker bases than NaOH, such as Et$_3$N, are unable to deprotonate QNZ, causing no change to its UV-Vis spectrum.

In the presence of Al(III) ions and OH$^-$, with the Al(III) equivalents lower than that of the base (typically 1/20/30 or 1/40/50 QNZ/Al^{3+}/OH$^-$ molar ratios), fluorescence was found to be reduced and this caused the quantum yield to decrease as well, as shown in Fig. 11 for QNZ/Al(acac)$_3$.[1]

[1] The quantum yield values have been calculated according to the following formula that accounts for changes in both absorbance and fluorescence areas [15]

$$\Phi_{\mathrm{QNZ/Al(III)}} = \frac{\text{fluorescence area}_{\mathrm{QNZ/Al(III)}} \times \mathrm{Abs}_{(\lambda_{exc})\mathrm{RhB}} \times n^2_{\text{solvent QNZ/Al(III)}}}{\text{fluorescence area}_{\mathrm{RhB}} \times \mathrm{Abs}_{(\lambda_{exc})\mathrm{QNZ/Al(III)}} \times n^2_{\mathrm{EtoH}}} \times \Phi_{\mathrm{RhB}}.$$

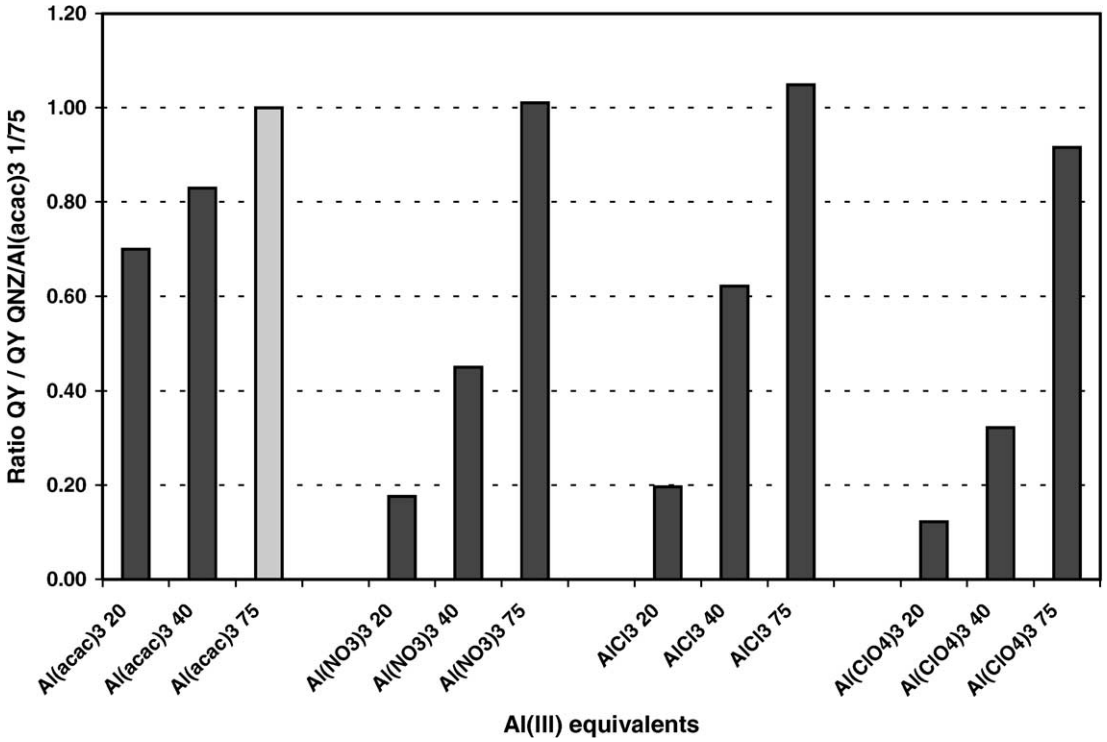

Fig. 10. Counterion effect for Al(III) salts in EtOH. The values are plotted relatively to the quantum yield of 1/75 QNZ/Al(acac)$_3$, which is shown in the bar with diagonal lines.

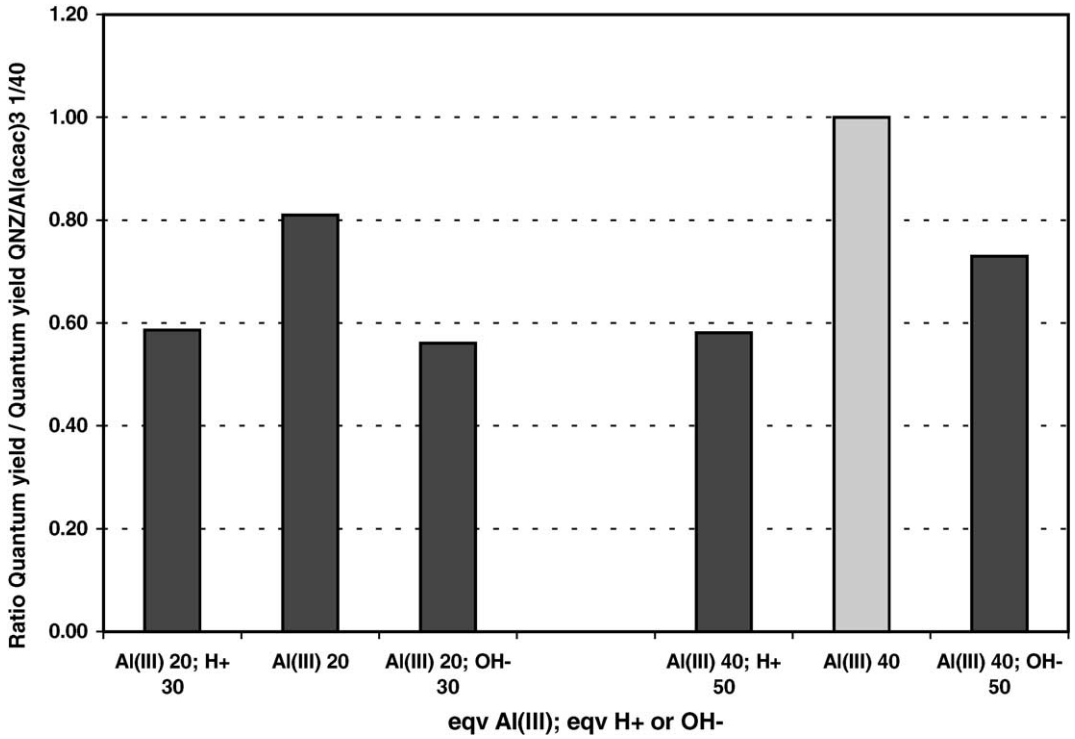

Fig. 11. pH effect on the quantum yield of QNZ/Al(acac)$_3$ in EtOH. The values are plotted relatively to the quantum yield of 1/40 QNZ/Al(acac)$_3$, which is shown in the bar with diagonal lines.

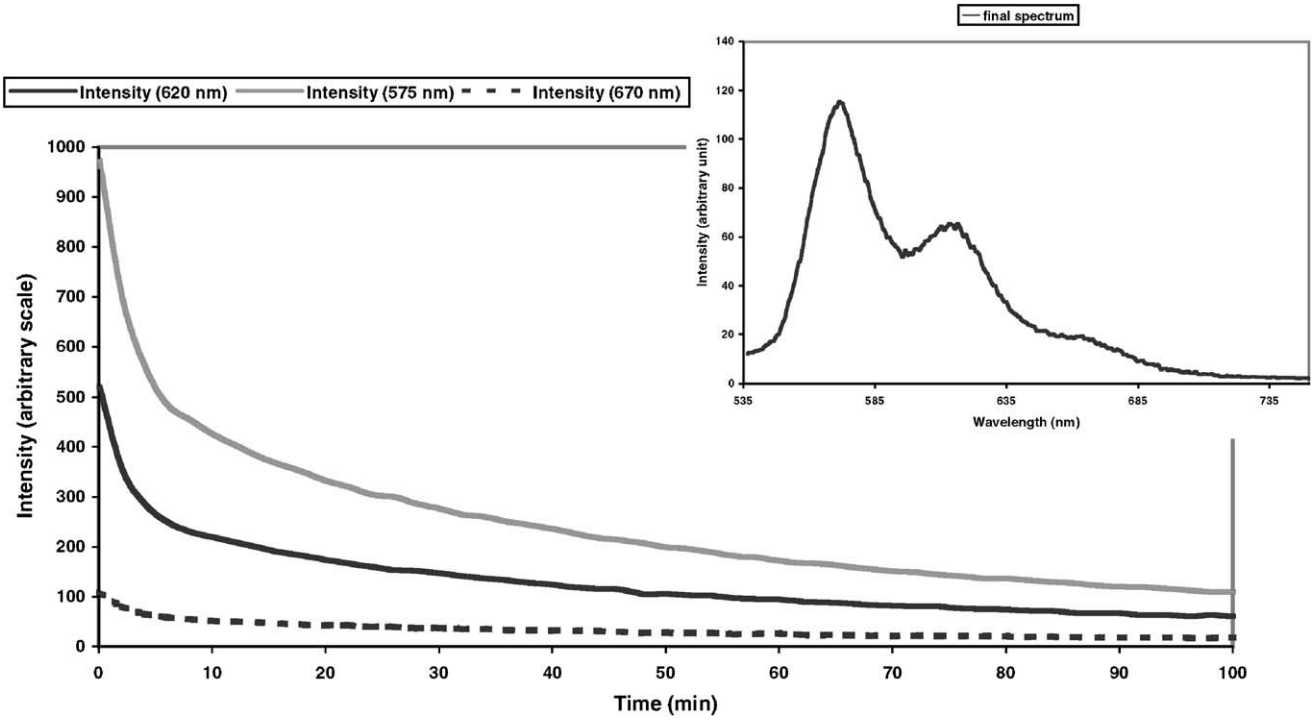

Fig. 12. Time decay of the fluorescence of 1/40 QNZ/Al(acac)$_3$ in EtOH due to the addition of 50 equiv. HCl.

The addition of HCl to QNZ, with QNZ/H^+ =1/7 molar ratio, caused, instead, no change in either the dye absorbance or its fluorescence properties. This confirmed that QNZ is generally present in solution in its protonated form.

In the presence of Al(III) ions and H^+, with QNZ/Al(III)/H^+ ratios of 1/20/30 or 1/40/50, a different behaviour was found with different Al(III) compounds. With Al(NO_3)$_3$ and Al(ClO_4)$_3$, the usual fluorescent species were obtained starting from both (i) QNZ/Al(III) and adding H^+; and (ii) QNZ/H^+ and adding Al(III). The overall effect of H^+ on the quantum yield was to increase it.

With Al(acac)$_3$ and H^+, instead, the formation of the strongly fluorescent species did not occur when Al(acac)$_3$, was added to QNZ/H^+ solutions. When H^+ was instead added to QNZ/Al(acac)$_3$, the solutions readily lost their pink colour and the fluorescence decayed as shown in Fig. 12. In the presence of H^+ and Al(acac)$_3$, the equilibrated solutions were light orange and their UV-Vis spectra showed a band centred at 555 nm; their fluorescence spectra had strongly reduced intensity. The overall effect was to reduce the fluorescence quantum yield as shown in Fig. 11. Therefore, acids have the effect of pushing back the complexation equilibrium between QNZ and Al(acac)$_3$.

2.8. Stability constants measurements

Quinizarin protonation constants and the stability constants of its Al(III) complexes were investigated potentiometrically in dioxane/water 80/20. Fig. 13 shows the QNZ titration curves. In the abscissa *B*/*L* is plotted, i.e. the number of moles of base over the number of moles of ligand. As Fig. 13 shows, the titration curve rises when *B*/*L* is −2 because QNZ contains two acidic protons. The protonation constants obtained through refinement of the titration data are reported in Table 3. The speciation curves (not shown) report protonated QNZ as the predominant species in solution until pH ∼ 4.5. At higher pH values, the monodeprotonated species started forming in solution. Nevertheless the formation of QNZ^{-H} never exceeded 70% and it is at his maximum for pH values around 10.7. Therefore QNZ^{-H} exists in solution always together with QNZ or QNZ^{-2H}. QNZ^{-2H} was found the predominant species in solution at pH values higher than 11. This speciation profile is in agreement with those reported in the literature [16].

Table 3
Comparison of quinizarin protonation constants measured in different solvents

Media	Dielectric constant (*D*)	log K_1	log K_2	Reference
Dioxane/water 4/1 (v/v)		10.39	9.93	This work
EtOH/H_2O 50/50 (v/v)		10.65	8.50	[17][a]
EtOH/H_2O 40/60 (v/v)		11.05	9.55	[18]
EtOH/H_2O 34/66 (v/v)	69	11.12	10.10	[19][a]
MeOH/H_2O 35/65 (v/v)	67	10.95	10.10	[19][a]
Acetone/H_2O 26/74 (v/v)	75	11.60	10.20	[19][a]
Ethylene glycol/H_2O 43/57 (v/v)	74	11.50	9.60	[19][a]
Glycerol/H_2O 46/54 (v/v)	76	10.60	9.46	[19][a]

[a] Determined by spectroscopic methods.

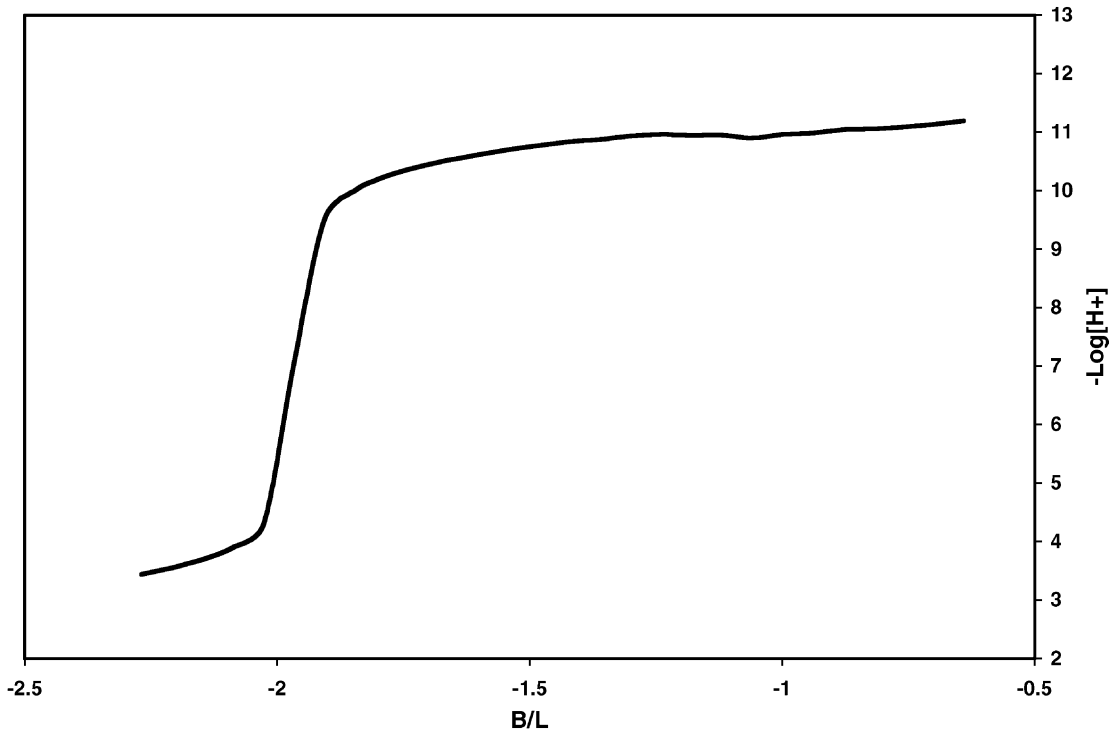

Fig. 13. Titration curves of QNZ with NaOH in dioxane/water 4/1 obtained in two different experiments.

The pK_a's obtained in this work in dioxane/water 80/20 are in good agreement with those reported in the literature for different media, as shown in Table 3 [17–19]. As expected, the log K_n values vary according to the protic character of the solvents in which they are measured. The deprotonation of hydroxyanthraquinones is known to increase proportionally to the proton-acceptor character of the solvents, as it can be seen with glycerol and ethylene glycol, while it decreases when the concentration of solvents such as MeOH or EtOH increases [19].

Further information on the species that form in the titrations was obtained with the on-line recording of UV-Vis spectra, using a spectrophotometer coupled to an automated titrator. The possibility of obtaining both stability constants and UV-Vis spectra from the same titration experiment was made difficult by the difference in the analyte optimal concentration required by the two experiments. In fact, reliable potentiometric data are obtained when the QNZ concentration is 10^{-3} M ca., while for reliable UV-Vis spectra a concentration of 10^{-4} M is desirable. The UV-Vis spectra

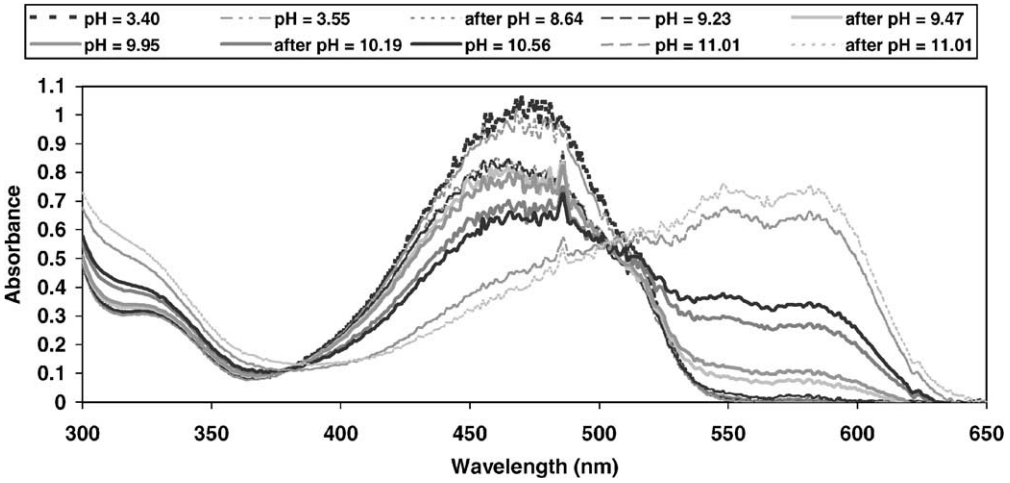

Fig. 14. UV-Vis spectra recorded during the titration of QNZ with NaOH in dioxane/water 80/20. Note: the noise in the spectra in intrinsic to the probe data recording.

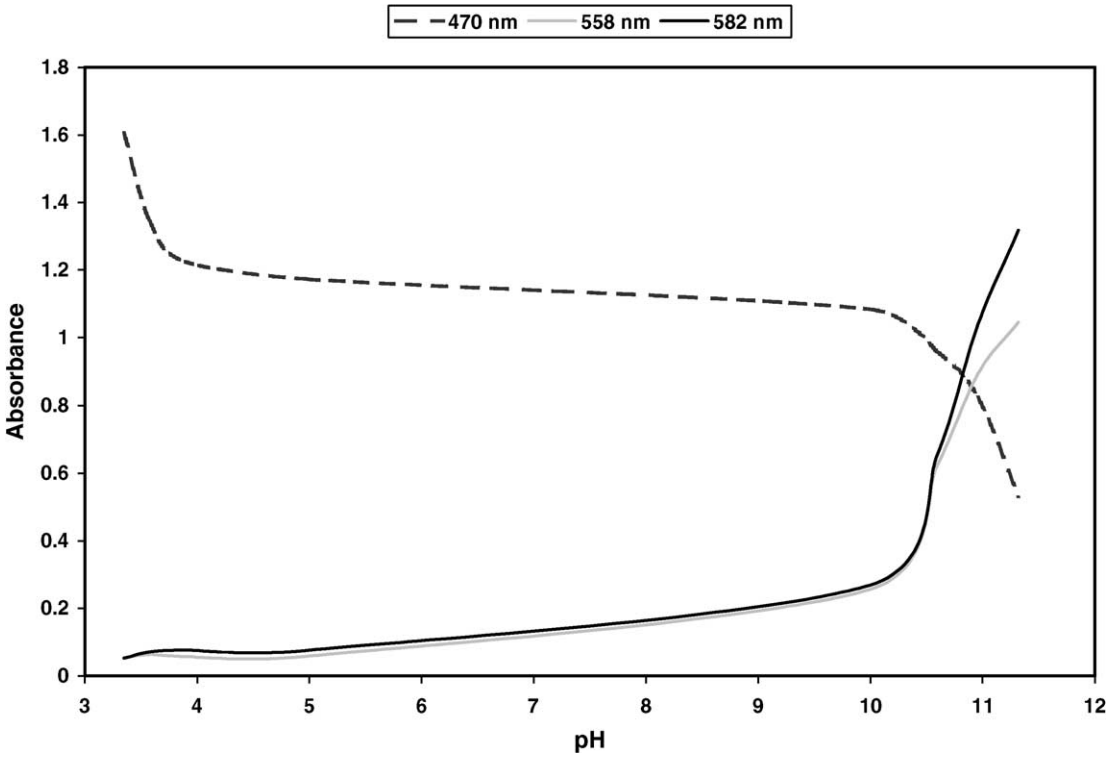

Fig. 15. Absorbance vs. pH for the titration of QNZ with NaOH.

recorded during the titration of quinizarin with NaOH are shown in Fig. 14. The titrations were followed spectrophotometrically between pH 3 and 11. In this pH range, the solutions of quinizarin changed colour from yellow to orange, then from red to pink and finally to violet. The initial acidic solution showed peaks at 280, 324, 473 and 575 nm. Increasing the pH the absorbance of the band at 473 nm progressively decreased while that of the band at 573 nm increased. From pH 10.1 onwards, another peak appeared at 550 nm and the intensity of the band at 280 nm decreased while that at 324 nm increased, becoming progressively a shoulder. At pH values higher than 11.1 (not shown in Fig. 14), the band at 580 nm had higher absorbance than that at 550 nm. An isosbestic point at 379 nm was observed in the pH range 3.4–11.0. These studies confirmed the results obtained while investigating the pH effect at high Al(III)/QNZ molar ratios.

The absorbance of the peaks that form and disappear during the titration of QNZ with NaOH, is plotted against the pH in Fig. 15. This graph confirms the reported speciation profile as three different slopes are found: up to pH 4; between pH 4 and 9; between pH 9.5 and 11. The literature reports similar studies in solutions of buffers and organic solvents where the shifting of the absorption maxima towards higher wavelengths takes place as a result of the transformation from QNZ to QNZ^{-H} [17,19,20]. The band shape and the pH at which this deprotonation takes place, are found to be largely affected by the nature and amount of organic solvent present. For example, in the absorbance versus pH

Table 4
Stability constants of the QNZ/Al(III) species measured potentiometrically in dioxane/water 80/20[a]

Complexation reactions		Stability constants ($\log \beta_{LMH}$)	Al(III)/QNZ 1/2 [QNZ] $\approx 2 \times 10^{-3}$ M
$Al^{3+} + 2QNZ + 2H_2O$	$[Al(QNZ^{-H})_2(H_2O)_2]^+ + 2H^+$	$\log \beta_{212}$	40.07
$Al^{3+} + 2QNZ + 2H_2O$	$[Al(QNZ^{-2H})(QNZ^{-H})(H_2O)_2] + 3H^+$	$\log \beta_{211}$	37.13
$Al^{3+} + 2QNZ + 2H_2O$	$[Al(QNZ^{-2H})_2(H_2O)_2]^- + 4H^+$	$\log \beta_{210}$	31.40
$Al^{3+} + 2QNZ + 2H_2O$	$[Al(QNZ^{-2H})_2(OH)(H_2O)]^{2-} + 5H^+$	$\log \beta_{21\text{-}1}$	26.60
$Al^{3+} + 2QNZ + 2H_2O$	$[Al(QNZ^{-2H})_2(OH)_2]^{3-} + 6H^+$	$\log \beta_{21\text{-}2}$	20.50

[a] β_{LMH} represents the overall stability constants for the protonated complexes such that β_{110} indicates the stability for the non-protonated species, ML. The overall stability constants correspond to $K_1, K_2, K_3, K_4, \ldots, K_n$, where K_n are the stepwise protonation constants defined as

$$K_n = \frac{H_nL^{(n-3)+}}{[H^+][H_{(n-1)}L^{(n-4)+}]}.$$

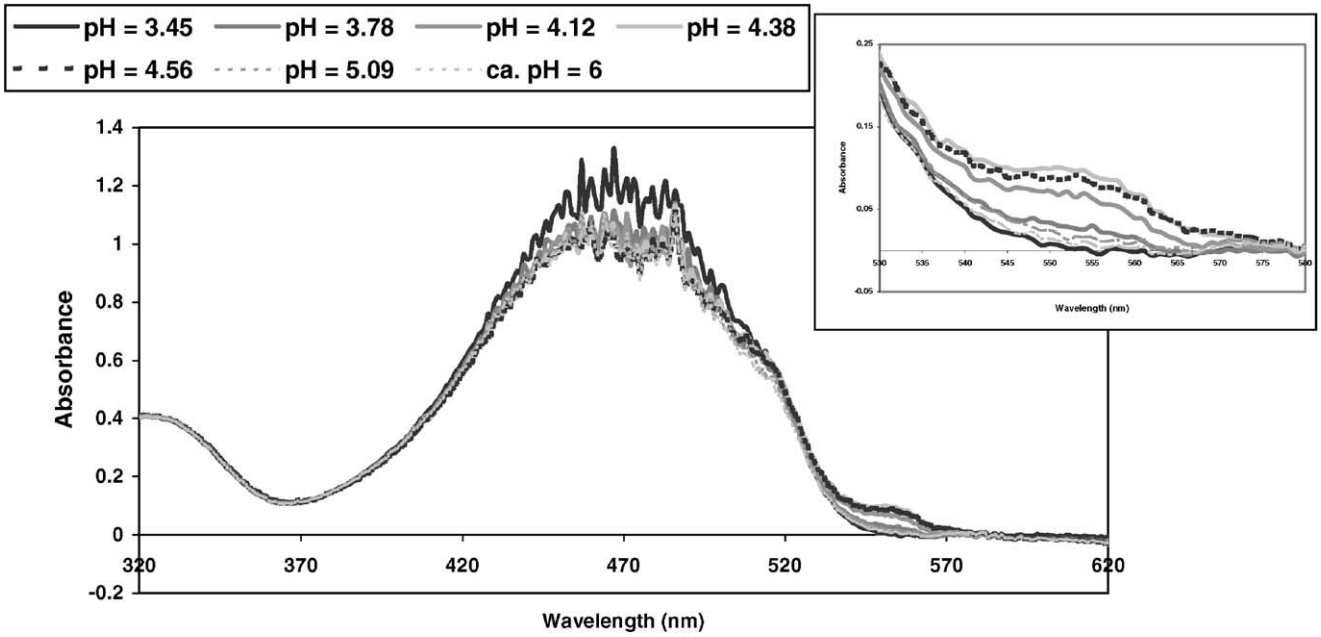

Fig. 16. UV-Vis spectra recorded during the titration of QNZ/Al$(NO_3)_3$ with NaOH in dioxane/water 80/20. Note: the noise in the spectra in intrinsic to the probe data recording.

plots the plateau is shifted to higher pH values with increasing amounts of MeOH or EtOH, whereas with glycerol and ethylene glycol it shifts towards lower pH values.

In the QNZ/Al$(NO_3)_3$ potentiometric titrations with NaOH, the metal-to-ligand ratio initially chosen was 1/3. However the refinement of these titration data was not successful. When instead 1/2 metal-to-ligand ratio was chosen, the stability constants reported in Table 4 were obtained ($\sigma = 0.66$). $\beta_{21\text{-}1}$ and $\beta_{21\text{-}2}$ correspond to species with 2/1 QNZ/Al(III) stoichiometry, that have lost, respectively, five and six protons. They are shown in Table 4 as involving the deprotonations of, respectively, one and two molecules of water as well as doubly deprotonated QNZ. Solvent of coordination is expected to complete the Al(III) six-coordination sphere in a 2/1 QNZ/Al(III) complex. This explanation finds confirmation in the pK_a values for these two dissociation steps that are, respectively, 5.80 and 6.10. Another possible explanation for $\beta_{21\text{-}1}$ and $\beta_{21\text{-}2}$ could involve the deprotonation of adjacent quinizarin molecules. The QNZ/Al(III) titrations with NaOH could be followed until ca. pH 6. At higher pH, a bright pink/red precipitate separated in the titration vessel. This material was too scarce to allow successful recovery and analysis.

During the titrations of QNZ/Al$(NO_3)_3$ with NaOH, the colour of the solutions changed from yellow to orange/red. The recorded UV-Vis spectra, for QNZ concentration of ca. 2×10^{-4} M, are shown in Fig. 16. The titrations were followed spectrophotometrically between pH 3 and 6, i.e. until precipitation occurred. The initial solution of Al(III)/QNZ showed bands at 280, 324, 466 and 518 nm. Increasing the pH until around 3.7 did not affect the spectra apart from a slight decrease in the absorbance of the band at 466 nm. When the pH was between 3.7 and 5.0, instead, another band formed centred at 553 nm. This band had its maximum of absorbance around pH 4.4 while at higher pH values it progressively decreased and it disappeared at pH 6.0, as shown in Fig. 17. These spectra are in agreement with those obtained with low Al(III) equivalents in the presence of H^+ ions.

2.9. Studies with OC_1C_{10}-PPV

The effect of QNZ/Al(acac)$_3$ on the fluorescence of OC_1C_{10}-PPV, was established in chloroform, using the following PPV/QNZ ratios/ 1/0.1, 1/1 and 1/5. In each case, Al(III) was added in solution in order to cover a wide range of ratios (1–75 relative to QNZ). At 490 nm excitation wavelength, the fluorescence spectra of PPV/QNZ 1/0.1 were dominated by PPV even at high Al(III) concentrations. With the other two stoichiometries, instead, the QNZ/Al(III) fluorescence became more predominant in the spectra proportionally to the Al(III) equivalents.

Using 490 nm as excitation wavelength, the presence of QNZ/Al(III) in solution did not produce any relevant increase in the PPV quantum yield. This is unsurprising as the excitation wavelength of QNZ/Al(III) and PPV are well separated (530 versus 490 nm). In this respect, it will be worthy of investigation the doping of a non-fluorescent polymer with the Al(III)/QNZ complexes.

2.10. Attempts of isolation of the fluorescent species

Attempts to isolate fluorescent species, from a wide range of QNZ/Al(III) stoichiometries, in the solid state have proved unsuccessful so far. Experiments have also been set

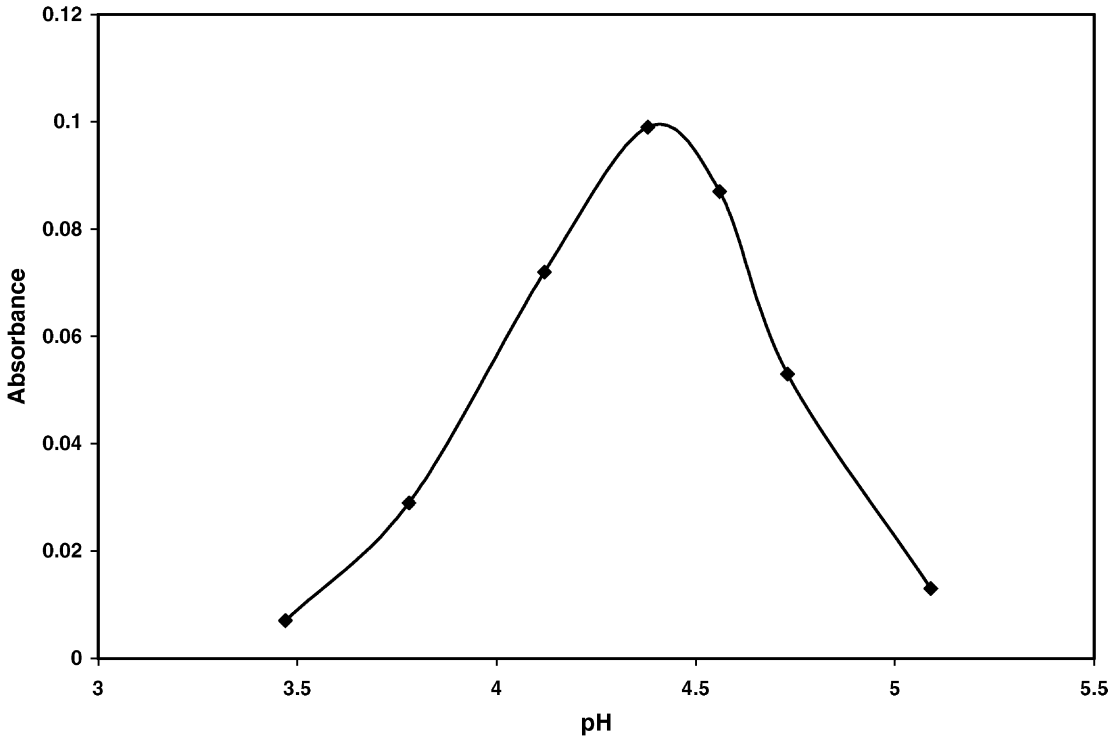

Fig. 17. Plot of the absorbance at 552 nm vs. pH for the titration of QNZ/Al$(NO_3)_3$ with NaOH.

up in the presence of a second ligand, namely py, $acac^-$, salicylaldehyde, salicylic acid, pyrophosphate, in order to form mixed-ligand complexes but these have also been proven unsuccessful.

In some instances single crystals were recovered but they either decomposed by loosing solvent on isolation or they proved to be unsuitable material for X-ray diffractometry.

3. Conclusions

Speciation studies suggest the supramolecular nature of the QNZ/Al(III) complexes as both the absorbance and fluorescence intensity of the complexes increases proportionally to the Al(III) equivalents up to 60/1 Al(III)/QNZ molar ratio and in certain cases even further.

Iso-propanol is the solvent that gives the highest quantum yield of fluorescence. With alcohols having higher polarity than *iso*-propanol, lower Φ values suggest that a certain degree of polarisation of the first excited singlet state is taking place.

The Al(III) counterion effect was also studied. Considering the different QNZ/Al(III) ratios investigated, Al$(acac)_3$ was the compound that overall gave the highest quantum yield values. This suggests that $acac^-$ plays an active role in stabilising the QNZ/Al(III) fluorescent species. The strong fluorescence reduction that occurs in the QNZ/Al$(acac)_3$ complexes in the presence of excess acid confirms this.

Potentiometric studies give QNZ protonation constant values in agreement with those reported in the literature. In the presence of Al$(NO_3)_3$, these studies could be performed only between pH 3 and 6 and the 2/1 QNZ/Al(III) species was found to be the most stable. Species involving the deprotonation of solvent molecules, or of adjacent QNZ molecules, also stem from these studies.

From the isolation attempts performed so far it appears that the formation of QNZ/Al(III) fluorescent species takes place mainly in solution and it suggests the direct participation of solvents in the stoichiometry of the fluorescent species. Our current inability to isolate the species had made identification difficult. From previous studies [12,13] it was suggested that a polymeric species of metal ions bonding to the ligand appears responsible in order to explain the apparent enhancement in quantum yield with metal ion concentration. Alternatively, the role of a supramolecular complex also appears possible where the metal ions are forming clusters with the ligand. Here the role and molecular size of the solvent play an important function in the competition and hence the quantum yield of fluorescence.

Finally, a preliminary investigation of the QNZ interaction with Ga(III) and In(III) shows that the latter metals are not as effective as Al(III) in forming fluorescent complexes. Boron is instead known to give strongly fluorescent species [3,4]. This suggests that the size, or the charge density, of the metal ions are important factor for the efficient formation of fluorescent complexes and

supramolecular complex formation. This will be reported on later.

4. Experimental

All the solvents and reagents were used as-purchased. An interval of time longer than 90 min passed between the preparation of the samples and the recording of UV-Vis and fluorescence spectra. UV-Vis spectra were recorded on a Hewlett Packard 8453 spectrophotometer. The concentration of the solutions was 3×10^{-5} M in QNZ.

Fluorescence spectra were measured on a Perkin-Elmer LS 55 Luminescence Spectrometer. Relative Φ values were measured at room temperature using 530 nm as excitation wavelength for $Al(acac)_3$ and 522 nm for $Al(NO_3)_3$, $AlCl_3$ and $Al(ClO_4)_3$. Some 490 nm was used as excitation wavelength in the studies with OC_1C_{10}-PPV. Rhodamine B in ethanol was used as reference ($\Phi = 0.70$) [15]. The concentration of the analysed solutions was 3×10^{-6} M in QNZ.

4.1. Potentiometric measurements

0.5 M Al(III) solutions were prepared from the nine hydrated nitrate salt, of analytical grade, with demineralised water. Solution temperatures were maintained at 25.0 ± 0.1 °C using a water-jacketed vessel while CO_2 was excluded by bubbling nitrogen. Ionic strength was maintained 0.10 M with $NaClO_4$. An amount of 50 ml of $\sim 10^{-3}$ M quinizarin, or QNZ/Al(III), in dioxane/water 4/1 (v/v) were titrated in the presence of excess $HClO_4$ (0.20 M) with standard 0.20 M NaOH. The 1/2 Al(III)/QNZ molar ratio was used.

Protonation and stability constants were calculated with HYPERQUAD [21]. Differences, in log units, between the values of β provide the stepwise protonation constants. The species considered were limited to those that could be justified by coordination chemistry. From the stability constants, the distribution curves for the species present at the equilibrium versus $-\log[H^+]$ were calculated with the program DISPLO [22].

Further information on the species that formed during the titrations was obtained with the on-line recording of UV-Vis spectra, using a Hewlett Packard 8453 spectrophotometer coupled to the titration automatic burette.

Acknowledgements

The authors wish to thank the EPSRC for funding through a ROPA award.

References

[1] R.S. Bottei, D.A. Lusardi, Thermochim. Acta 43 (1981) 355.
[2] H. Drechsel, M.M.L. Fiallo, A. Garnier-Suillerot, B.F. Matzanke, V. Schünemann, Inorg. Chem. 40 (2001) 5324.
[3] A. Gomez-Hens, M. Valcárcel, Analyst 107 (1982) 465.
[4] M.R. Ceba, A. Fernandez-Gutierrez, C.M. Sanchez, Microchem. J. 32 (1985) 286.
[5] J. Sharma, H.B. Singh, T.S. Rao, Curr. Sci. 55 (1986) 345.
[6] R. Kiraly, R.B. Martin, Inorg. Chim. Acta 67 (1982) 13.
[7] P.H. Merrell, Inorg. Chim. Acta 32 (1979) 99.
[8] M. Roman, A. Fernandez-Gutierrez, J. Suarez, F. Ales, Microchem. J. 34 (1986) 270.
[9] H.D. Coble, H.F. Holtzclaw, J. Inorg. Nucl. Chem. 36 (1974) 1049.
[10] J. Sharma, H.B. Singh, Inorg. Chim. Acta 133 (1987) 161.
[11] M.J. Maroney, R.O. Day, T. Psyris, L.M. Fleury, J.P. Whitehead, Inorg. Chem. 28 (1989) 175.
[12] N.S. Allen, G. Hayes, P.K. Riley, A.M. Richards, J. Photochem. 38 (1987) 365.
[13] N.S. Allen, A.M. Richards, Eur. Polym. J. 26 (1990) 1229.
[14] M.B. Ledger, P. Suppan, Spectrochim. Acta 23A (1967) 641.
[15] J.N. Demas, G.A. Crosby, J. Phys. Chem. 75 (1971) 991.
[16] J. Barbosa, J. Sanchez, E. Bosch, Talanta 31 (1984) 279.
[17] H. Sadeira, K.A. Idriss, M.M. Seleim, M.S. Abdel-Aziz, Monatsh 129 (1998) 49.
[18] K.A. Idriss, M.M. Seleim, A.S. El-Shahawy, M.S. Saleh, H. Sadeira, Monatsh 119 (1988) 683.
[19] K.A. Idriss, I.M. Issa, R.M. Issa, A.M. Hammam, Indian J. Chem. 14B (1976) 117.
[20] M.E. Bodini, V. Arancibia, Polyhedron 10 (1991) 1929.
[21] A. Sabatini, A. Vacca, P. Gans, Coord. Chem. Rev. 120 (1992) 389.
[22] A. Sabatini, A. Vacca, P. Gans, Private communication.